SCIENTIFIC REPORTS

OPEN

SUBJECT AREAS:
MICRORESONATORS
NANOPHOTONICS AND PLASMONICS

Received
10 September 2013

Accepted
9 December 2013

Published
16 January 2014

Correspondence and requests for materials should be addressed to J.W. (jwang@hust.edu.cn)

* Current address: Department of Information Engineering, The Chinese University of Hong Kong, Shatin, N.T., Hong Kong, China.

# Proposal and numerical study of ultra-compact active hybrid plasmonic resonator for sub-wavelength lasing applications

Chao Xiang[1]*, Chun-Kit Chan[2] & Jian Wang[1]

[1]Wuhan National Laboratory for Optoelectronics, School of Optical and Electronic Information, Huazhong University of Science and Technology, Wuhan 430074, Hubei, China, [2]Department of Information Engineering, The Chinese University of Hong Kong, Shatin, N.T., Hong Kong, China.

**We design an ultra-compact active hybrid plasmonic ring resonator for lasing applications at deep sub-wavelength scale. The combined contributions of hybrid plasmonic mode, circular-shaped cross section of nanowire, and ring resonator structure with round-trip whispering-gallery cavity, benefit reduced metallic absorption loss, tight mode confinement, enhanced cavity feedback, achieving high quality factor ($Q$), small mode volume ($V$), high Purcell factor ($F_p$), low threshold gain ($G_{th}$), and ultra-small footprint with sub-micron size. The performance dependence on the geometrical parameters, including gap height ($H_g$), cross section radius ($R_c$), and ring radius ($R_r$), are comprehensively analyzed, showing high $Q$ factor of 1650 ($H_g$=30 nm, $R_c$=100 nm, $R_r$=800 nm), ultra-small mode volume of 0.0022 μm$^3$ ($H_g$=5 nm, $R_c$=100 nm, $R_r$=800 nm), cut off of all photonic modes for pure plasmonic mode lasing with $R_c$<70 nm ($H_g$=10 nm, $R_r$=800 nm), maximum Purcell factor of 813 and minimum threshold gain of 1407 cm$^{-1}$ ($H_g$=5 nm, $R_c$=50 nm, $R_r$=400 nm). The general design rules of the presented hybrid plasmonic ring resonator provide the potential to further extend ultra-compact sub-micron lasing applications (i.e. different lasing wavelength band) with proper choice of gain materials and geometric structures.**

The coherent light source plays an important role in tremendous scientific areas ranging from optical communications, bio-photonics to quantum optics. In recent years, various types of coherent light laser sources with the size of micrometers or nanometers have been proposed[1,2], which have paved a way towards the future on-chip integrated photonic applications. Such kind of devices feature enhanced light-matter interaction and strong feedback mechanism. For instance, resonant structures with a high quality ($Q$) factor can greatly upgrade the interaction and feedback, resulting in the reduction of the functioning threshold[3]. However, resonant geometries such as ring resonators and disks usually require a relatively large size and thus increase the component footprint[4]. In addition, a large component size not only increases the physical dimension, but also tends to bring in a large mode volume ($V$), which is undesirable in micro/nano lasing applications. To be compatible with the trend of high-density integration, a laudable goal for resonators used in micro/nano lasing applications is to achieve a high $Q$ factor while maintaining a small mode volume.

Surface plasmon polaritons (SPP), the collected charge oscillations along the interface between the dielectric and metallic media, can break the diffraction limit and has great potential in applications where light can be generated and manipulated at sub-wavelength scale[5]. Owing to the ability of confining mode energy into an ultra-small area (less than $(\lambda/2n)^3$), SPP-based light emitters have attracted increasing interest, such as metal-cavity shield laser[6], surface plasmon amplification by stimulated emission of radiation (SPASER) based nanolaser[7], etc. However, due to metallic absorption loss, SPP-assisted lasers usually require high gain to compensate the absorption loss for success in lasing operations. Specifically, a hybrid plasmonic waveguide was proposed to reduce the absorption loss while offering a strong mode confinement[8]. A plasmon laser was then demonstrated when a semiconductor nanowire was incorporated[2]. In such kind of plasmon laser, the feedback mechanism is based on a Fabry-Pérot cavity. The end-facets of the nanowire provide the refection and feedback necessary for lasing. However, the small reflectivity and mirror loss for such structures give limited $Q$ factor. The use of round-trip whispering-gallery cavity could improve the $Q$ factor performance[9], but little attention has been put to lasing applications.

In this paper, we propose a simple active hybrid plasmonic ring resonator which supports whispering-gallery-like hybrid plasmonic modes. Finite-element method (FEM) is used to comprehensively characterize the mode properties ($Q$ factor, mode volume, Purcell factor, threshold gain) and their device parameters (gap height $H_g$, cross section radius $R_c$, ring radius $R_r$).

## Results

**Design of active hybrid plasmonic ring resonator.** Fig. 1(a) shows the structure of our proposed active hybrid plasmonic ring resonator. A semiconductor nanowire with circular cross section (radius $R_c$) is designed in a ring shape with a radius of $R_r$. The ring shaped nanowire is placed on a metal substrate insulated by a thin low-index dielectric layer. Fig. 1(b) illustrates the cross section, where the low-index dielectric layer forms a gap between the semiconductor nanowire and the metal substrate with a height of $H_g$.

Here we chose Cadmium Sulfide (CdS), Magnesium Floride ($MgF_2$) and Silver (Ag) as the semiconductor, the low-index dielectric and the metal material, respectively. We calculated the mode distribution of the cross section at the lasing wavelength of CdS nanowire (~490 nm). In our simulations, silver was modeled by Drude model and the permittivities of CdS and $MgF_2$ were chosen as 5.76 and 1.96, respectively[2,10].

**Mode properties.** In the designed hybrid structure, two major modes are supported: the hybrid plasmonic (HP) mode and the fundamental photonic (PH) mode. The HP mode can be regarded as a kind of supermode, which is formed by the combined contributions from SPP and discontinuity of electric field at the interface between low-index gap layer ($MgF_2$) and high-index nanowire (CdS). The HP mode is also known from the coupling between in-phase fundamental photonic mode and surface plasmon mode[11]. The PH mode is very similar to the traditional fundamental guiding mode confined in the high-index region. Other possibly supported modes in the hybrid structure include i) supermode from coupling between out-of-phase fundamental photonic mode and surface plasmon mode[11]; ii) high-order photonic modes with large nanowire cross section radius $R_c$; iii) supermodes from coupling between high-order photonic modes and surface plasmon mode. When optimizing the structure with expected superior performance such as small mode volume with small nanowire cross section radius, these other modes rather than HP mode and PH mode are not considered here for simplicity as they are more easily cut off and not of interest for the desired ultra-compact sub-wavelength lasing applications. The cross section views of the on-resonance (~490 nm) energy density distributions ($H_g$=10 nm, $R_c$=100 nm, $R_r$=800 nm) for the HP mode and the PH mode are depicted in Fig. 1(c) and (d), respectively. As expected, the HP mode peaks in the gap region and a part of the mode has an overlap with the nanowire, which provides the lasing gain. By contrast, the PH mode is mainly distributed in the nanowire, showing a relatively larger mode size and has less overlap with the metal substrate. This indicates that the HP mode features smaller mode volume but may be more vulnerable to the metal absorption loss. Moreover, the contour plots of energy density, as depicted in Fig. 1(c) and (d), show that the energies of both HP and PH modes slightly extends outwards, which can be ascribed to the bending radiation effect. To further show the influence of the gap layer and the ring structure on the HP mode distribution, which is used in lasing applications, we plot the normalized energy density distribution along y (r=800 nm) and radial (y=15 nm) directions, as shown in Fig. 1 (e) and (f), each corresponding to the vertical and horizontal blue lines marked in Fig. 1(c), respectively. Along the y direction, the mode energy density features a sharp peak in the gap layer region. Along the radial direction, the mode energy density profile within the nanowire region is Gaussian-like with a width of only ~50 nm, which is determined by the physical dimension of the nanowire in this direction. Meanwhile, at symmetric positions with respect to the center vertical axis of the nanowire, the outer branch (close to the outer rim of the ring resonator) has higher energy density, indicating more energy is confined at the outward parts of the ring resonator.

**Impact from gap height $H_g$.** The operation performance of the designed active hybrid plasmonic ring resonator is mainly influenced by the following three geometrical parameters: (1) gap height $H_g$; (2) cross section radius $R_c$; and (3) ring radius $R_r$.

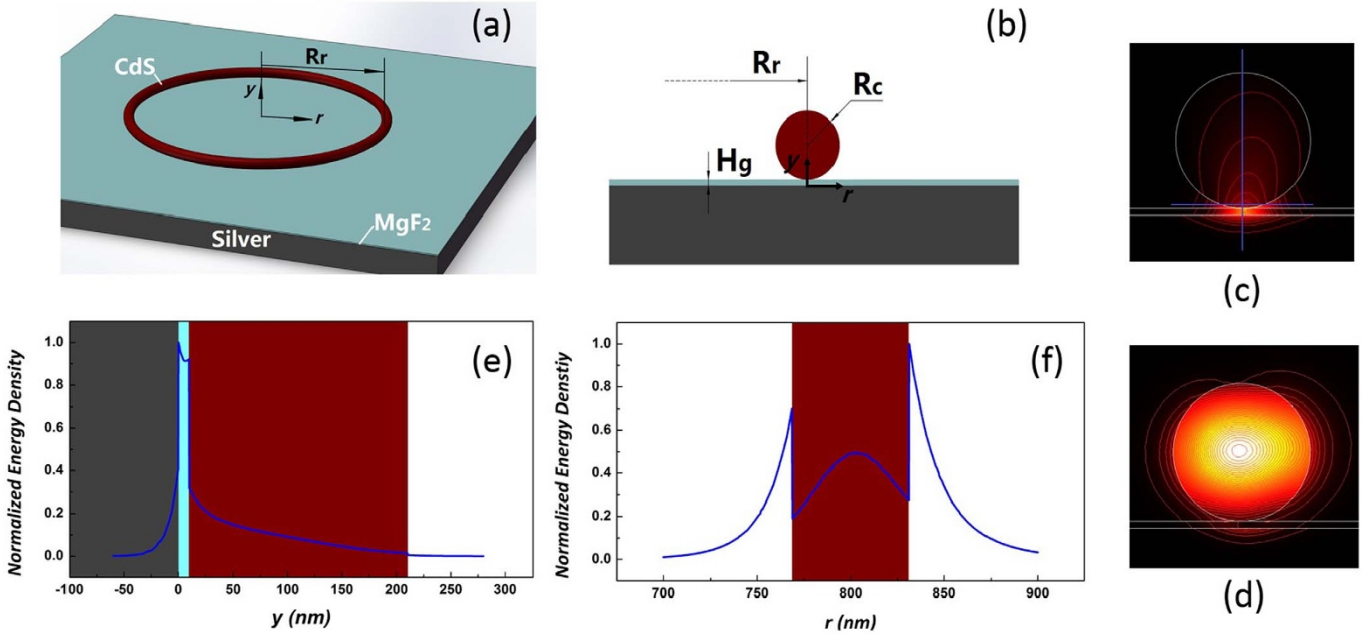


**Figure 1** | (a) 3-D illustration of the proposed active hybrid plasmonic ring resonator. (b) The cross section view of the hybrid plasmonic ring resonator. (c)(d) The energy flux density distribution for HP mode (d) and PH mode (e) respectively. (e)(f) The normalized energy flux density for HP mode along the $y$ (e) and $r$ (f) directions.

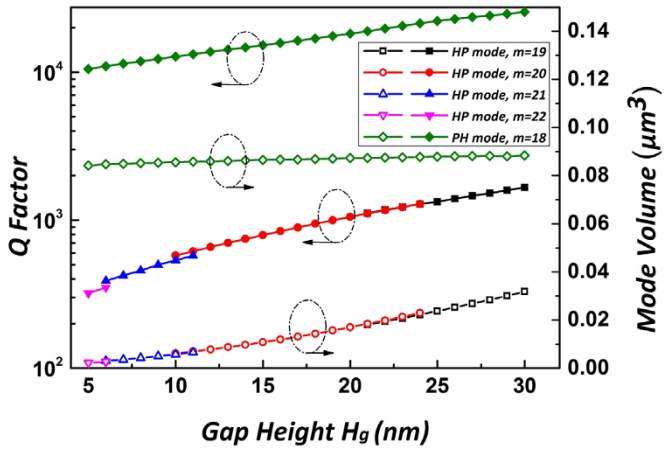


**Figure 2 | Q factor and mode volume versus gap height *Hg* at a resonance in the CdS lasing band for HP mode and PH mode (*Rc*=100 nm, *Rr*=800 nm).**

From the mode distribution shown in Fig. 1(c), it is expected that the low-index gap layer between the nanowire and metal substrate plays an important role in the HP mode properties. Fig. 2 shows the dependence of the *Q* factor and the mode volume (*V*) on the gap height for both HP and PH modes at a resonance in the lasing wavelength band[12] ($R_c$=100 nm, $R_r$=800 nm). With an increase of gap height from 5 to 30 nm, the *Q* factor increases from 300 to 1650 for the HP mode, due to less mode energy distributed in the silver substrate and the resultant low absorption loss. For the PH mode, the *Q* factor also increases as the gap height increases. Such phenomenon can be briefly explained as follows. When the nanowire is lifted away from the metal substrate, less mode energy leaks into the metal substrate, resulting in the reduction in the total loss of the resonator and the increase in the *Q* factor. Since the HP mode is tightly confined in the small gap region, the mode volume can be ultra-small (around 0.0022 $\mu m^3$) at sub-wavelength scale under a small a gap height of 5 nm. The mode volume changes from 0.0022 to 0.0318 $\mu m^3$ as the gap height increases from 5 to 30 nm. In addition, the mode volume of the PH mode, as shown in Fig. 2, remains almost unchanged (0.0842–0.0884 $\mu m^3$), showing larger mode volume compared to the HP mode and less dependency of mode volume of the PH mode on the gap layer.

**Impact from cross section radius *Rc*.** For the PH mode, it is well known that the mode confinement mechanism relies on the refractive index difference between the guiding nanowire and the surrounding air (or $MgF_2$ under the nanowire). In general, it is difficult to shrink the size of the PH mode at subwavelength scale by reducing the physical dimension of the nanowire due to the diffraction limit. By comparison, the HP mode holds the potential to break the diffraction limit thanks to the partial contribution from plasmonics. To clearly show the impact of diffraction limit on both PH and HP modes, we comprehensively investigate the dependence of the PH and the HP mode properties on the cross section radius $R_c$ of the nanowire, and the results are depicted in Fig. 3(a) and (b) ($H_g$=10 nm, $R_r$=800 nm).

Fig. 3(a) plots the effective refractive index ($n_{eff}$) of the HP and the PH modes, as a function of the cross section radius $R_c$, for different mode numbers that may have resonance in the lasing wavelength band[12]. Several important conclusions can be drawn from Fig. 3(a). First, there exists a cut-off effective refractive index at ~1.185 for the HP mode and ~1.283 for the PH mode. Second, one can see that the PH mode cannot exist when the cross section radius $R_c$ is smaller than 70 nm. Such phenomenon can be explained with the fact that the confinement mechanism of the PH mode is broken at such small geometrical dimensions, due to the diffraction limit, resulting in the evanescence of the PH mode and prohibiting the photonic lasing of the PH mode at such deep subwavelength scale. This cut-off radius of 70 nm, compared to the previously reported cut-off radius value of 65 nm[9], is slightly larger, which is a result of the bending effect of nanowire ring resonator and the resultant radiation loss. In particular, the cut-off radius of 70 nm for the PH mode implies both HP and PH modes lase at $R_c$>70 nm while only the HP mode lases at $R_c$<70 nm, which offers a theoretical basis to remove PH mode lasing and thus achieves pure HP mode lasing. Third, the HP mode is still available even under a small cross section radius $R_c$ of 20 nm, showing its ability to break the diffraction limit. Fourth, with the decrease of cross section radius $R_c$, the whispering-gallery-like mode with a smaller azimuthal mode number disappears first for both HP and PH modes. For instance, the mode number of the supported PH modes follows m≥8 at $R_c$=130 nm and m≥13 at $R_c$=75 nm. It is clearly shown that the PH modes with mode number of m=8, 9, 10, 11, 12, 13 vanish one after another as the cross section radius $R_c$ is reduced below 130, 115, 100, 90, 85, 75 nm, respectively. Additionally, the mode number of achievable HP modes becomes m≥7 at $R_c$=60 nm and m≥12 at $R_c$=25 nm. Specifically, the HP modes with mode number of m=7, 8, 9, 10, 11, 12 disappear one by one as reducing the cross section radius $R_c$ below 60, 50, 40, 35, 30, 25 nm, respectively. Fifth, although Fig. 3(a) shows a limited number of HP modes (m=7→m=20) and PH modes (m=8→m=20) that may have resonance in the lasing wavelength band, the HP modes (m<7, m>20) and the PH modes (m<8, m>20) are also possible in principle. However, the lower limit of mode number of the HP and the PH modes is dependent on the cross section radius $R_c$. HP and PH modes with small mode number are gradually cut off as reducing the cross section radius $R_c$. As shown in Fig. 3(a), one can see that the available mode number values of m>8 for the PH modes at $R_c$<130 nm and m>7 for HP modes at $R_c$<60 nm.

The cut-off phenomenon related to geometrical dimensions offers design guidelines of ring resonators to support pure tightly confined HP modes and select desired mode number of the HP modes. According to the relationship of $2\pi R_r n_{eff} = m\lambda$ between effective refractive index ($n_{eff}$), mode number ($m$) and resonance wavelength ($\lambda$) for whispering-gallery-like HP and PH modes, we further show in Fig. 3(b) the resonance wavelength as a function of the cross section radius $R_c$ for the supported HP and PH modes, putting another straightforward way to find lasing applications for ring resonators. One can easily draw several important points from Fig. 3(b) as follows. 1) Cut-off of all PH modes (critical cross section radius $R_c$=70 nm): all PH modes are cut off at $R_c$<70 nm and pure HP modes are achievable. 2) Trend of mode number-dependent resonance wavelength: the resonance wavelength decreases as increasing the mode number for a given cross section radius $R_c$. 3) Range of resonance wavelength (cut-off of small mode number of HP and PH modes): owing to $R_c$-dependent lower limit of mode number of the HP and PH modes, as shown in Fig. 3(a), there always exists a maximum wavelength (upper limit) corresponding to the supported minimum mode number (lower limit) of the HP and PH modes at a given cross section radius $R_c$. For example, as shown in Fig. 3(b), the upper limit resonance wavelength of the HP mode is 440 nm (m=14) at $R_c$=20 nm, 661.6 nm (m=9) at $R_c$=40 nm and 866.3 nm (m=7) at $R_c$=60 nm. For PH mode, the upper limit resonance wavelength is 464.3 nm (m=14) at $R_c$=70 nm, 645.6 nm (m=10) at $R_c$=100 nm and 823.2 nm (m=8) at $R_c$=130 nm. In particular, we further deduce two fitting curves for the HP mode ($\lambda$ (nm) = 10.2 × $R_c$ ($nm$) + 242.3) and the PH mode ($\lambda$ (nm) = 5.79 × $R_c$ ($nm$) + 57.9), showing $R_c$-dependent upper limit of the wavelength range (dashed curves in Fig. 3(b)). 4) Considering the use of CdS as the gain material for lasing applications, the possible lasing wavelength band of 489–510 nm for CdS is marked (gray bar) in Fig. 3(b). One can clearly see that the cross section radius $R_c$ is desired to be larger than 75 nm for possible PH mode lasing applications

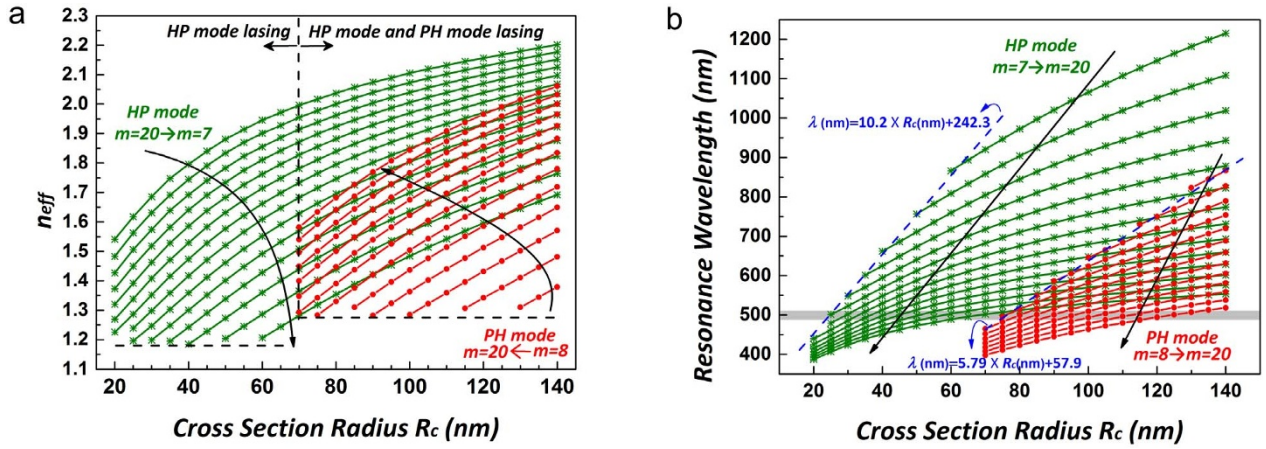


**Figure 3** | (a) Effective refractive index ($n_{eff}$) and (b) resonance wavelength versus cross section radius *Rc* for HP mode and PH mode (*Hg*=10 nm, *Rr*=800 nm).

(i.e. resonance wavelength sitting in the gray bar region). Similarly, $R_c$>25 nm is preferred to enable potential HP mode lasing applications. In order to facilitate pure HP mode lasing applications, the available range of the cross section radius $R_c$ is 25 nm<$R_c$<70 nm. Additionally, the narrow gray bar region (489–510 nm for CdS), as shown in Fig. 3(a), implies possible single pure HP mode lasing applications. Remarkably, Fig. 3(a) and (b) imply a general approach to fully characterize the operation performance of an active hybrid plasmonic ring resonator for lasing applications which can be independent of the adopted materials. That is, for different lasing applications with different materials, similar results as in Fig. 3(a) and (b) can be obtained, indicating critical cross section radius $R_c$ with all PH modes cut off (pure HP modes), upper limit of wavelength range (lower limit of mode number) with HP modes having small mode number cut off at a given cross section radius $R_c$, and available range of cross section radius $R_c$ for specific lasing wavelength applications.

**Impact from ring radius $R_r$.** For the proposed active hybrid plasmonic ring resonator with $R_c$<70 nm that supports only pure HP mode lasing with all PH modes cut off, another important geometrical parameter beyond gap height $H_g$ and cross section radius $R_c$ is the ring radius $R_r$ of the ring resonator. *Q* factor and mode volume are two key parameters of a ring resonator, especially at subwavelength scale. Specifically, when considering lasing applica tions for a resonator or a cavity, a high Purcell factor and a low threshold gain are preferred[2]. We further study in Fig. 4(a) and (b) the impact of the ring radius $R_r$ on Q factor, mode volume, Purcell factor and threshold gain ($H_g$=5 nm, $R_c$=50 nm). *Q* factor and mode volume as a function of ring radius $R_r$ are shown in Fig. 4(a). Considering an ideal case and ignoring the scattering loss due to fabrication-induced surface roughness for simplicity, the total *Q* factor of the ring resonator ($Q_{total}$) is influenced by the radiation loss ($Q_{rad}$) and material absorption loss, mainly from the metal ($Q_{abs}$), fulfilling a relationship of $1/Q_{total}=1/Q_{rad}+1/Q_{abs}$. The impact of radiation loss of the ring resonator is weighed by $Q_{rad}$, which takes into account only the geometry-related radiation loss by removing the absorption part of the material. The impact of material absorption loss is weighed by $Q_{abs}$. As expected, $Q_{rad}$ increases quickly from 250 to 113150 when $R_r$ is changed from 300 to 800 nm, showing a significant reduction in radiation loss of the ring resonator under a relatively larger ring radius $R_r$. As shown in Fig. 4(a), the total *Q* factor is determined by the radiation loss under a small ring radius ($R_r$<400 nm) but is dominated by the absorption loss under a large ring radius ($R_r$>400 nm). Meanwhile, a large ring radius $R_r$ also results in a large mode volume. With the increase of ring radius $R_r$ from 300 to 800 nm, the mode volume increases from $5.44\text{x}10^{-4}$ to $1.37\text{x}10^{-3}$ μm³.

For lasing applications, a higher Purcell factor and a lower threshold gain are required to enable efficient cavity feedback and high lasing efficiency. Figure 4(b) shows the ring radius $R_r$ dependent Purcell factor and threshold gain. It is noted that the Purcell factor ($F_p$) reaches its maximum value of 813 at $R_r$=400 nm, where the highest *Q* factor meets a relatively small mode volume shown in Fig. 4(a). The threshold gain, which is inversely proportional to the *Q* factor, gains its minimum value of 1400 $cm^{-1}$ at $R_r$=400 nm. A relatively low threshold gain ranging from 1407 to 3187 $cm^{-1}$ can always be achieved when the ring radius $R_r$ is at sub-micron size varying from 300 to 800 nm[13,14]. The obtained results shown in Fig. 4(b) imply that an ultra-compact laser with sub-wavelength scale could be potentially available using active hybrid plasmonic ring resonator with a relatively low threshold gain.

## Discussion

We present a design of ultra-compact active hybrid plasmonic ring resonator for sub-wavelength lasing applications. The performance parameters including *Q* factor, mode volume, Purcell factor and threshold gain are analyzed. The geometrical parameters such as gap height $H_g$, cross section radius $R_c$ and ring radius $R_r$ affecting operation performance are discussed. The obtained results show: 1) high Q factor of 1650 at $H_g$=30 nm and ultra-small mode volume of 0.0022 μm³ at $H_g$=5 nm ($R_c$=100 nm, $R_r$=800 nm); 2) critical cross section radius $R_c$=70 nm for cut-off of all PH modes ($R_c$<70 nm: pure HP modes) and available range from 25 to 70 nm of cross section radius $R_c$ for lasing applications with wavelength within 489–510 nm (CdS) ($H_g$=10 nm, $R_r$=800 nm); 3) maximum Purcell factor of 813 and minimum threshold gain of 1407 $cm^{-1}$ at $R_r$= 400 nm and low threshold gain within 1407–3187 $cm^{-1}$ under sub-wavelength $R_r$ within 300–800 nm ($H_g$=5 nm, $R_c$=50 nm).

As well known, the *Q* factor of conventional plasmonic ring resonators is mainly restricted by the huge metallic absorption loss. Since hybrid plasmonic structures reduce the absorption loss while maintaining remarkably tight mode confinement, it is possible to greatly improve the *Q* factor of the active hybrid plasmonic ring resonators without sacrificing too much on the mode volume performance. Moreover, high Purcell factor and low threshold gain are also available owing to the achievable high *Q* factor and low mode volume using active hybrid plasmonic ring resonators. Remarkably, HP modes receiving more interest in active hybrid plasmonic ring resonators feature hybrid properties of plasmonic mode and dielectric mode. The properties of HP modes are sensitive to geometrical parameters including gap height $H_g$, cross section radius $R_c$ and ring

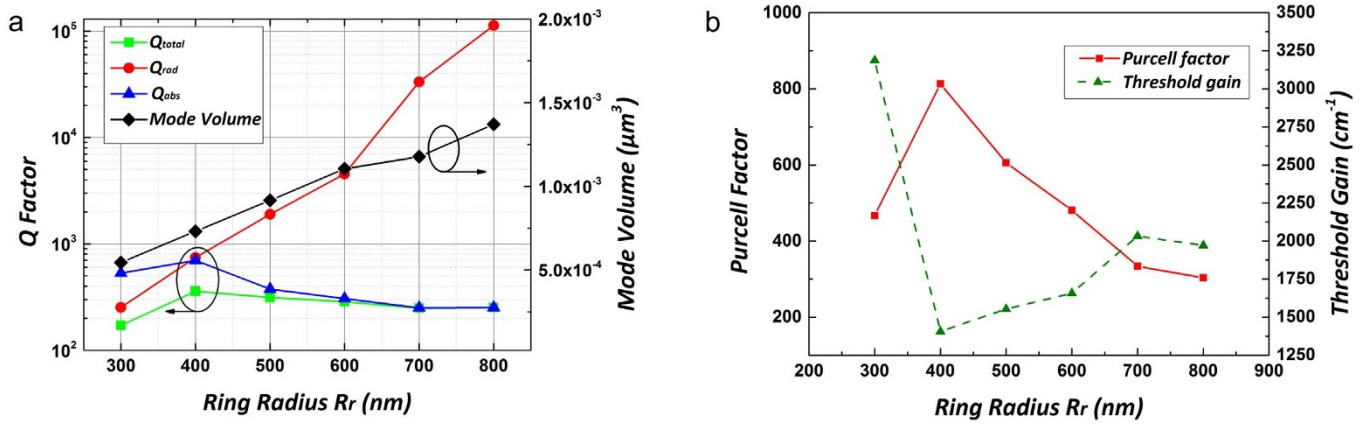


**Figure 4** | (a) $Q_{total}$, $Q_{rad}$, $Q_{abs}$, mode volume and (b) Purcell factor and threshold gain versus ring radius $Rr$ for HP mode ($Hg$=5 nm, $Rc$=50 nm).

radius $R_r$ which influence the operation performance in different ways.

The gap height $H_g$ determines the hybridization of the plasmonic mode and the dielectric mode. When the gap height $H_g$ is small, the HP mode is more plasmonic mode-like with large absorption loss (low $Q$ factor) but tight mode confinement (small mode volume). When the nanowire is lifted away from the metal substrate by a large gap height $H_g$, the HP mode tends to be more dielectric mode-like with high $Q$ factor and large mode volume. To get a better balance between the absorption loss and mode confinement, it is preferred to optimize the hybridization level of plasmonic mode and dielectric mode, i.e. gap height engineering for high $Q$ factor and relatively small mode volume.

The cross section radius $R_c$ mainly determines the mode cut off properties. Due to the diffraction limit and mode guiding mechanism, PH modes cannot exist when the cross section radius $R_c$ is reduced below a certain value. In practical lasing applications, the interesting cut off phenomenon of all PH modes can benefit pure HP mode lasing without the mode competition from PH modes. In addition to the cut off of all PH modes, the cross section radius $R_c$ also impacts on the cut off of PH modes with small mode number, setting the upper limit of achievable resonance wavelength range for a given $R_c$.

The ring radius $R_r$ then determines the radiation loss induced by the bending effect of ring-shaped resonators. Due to the bending radiation, the PH mode of a ring resonator is more easily cut off compared to that of a straight waveguide[2,9]. Meanwhile, for HP modes, the radiation has a large impact on $Q_{rad}$ (dielectric mode part), but contribute less to $Q_{abs}$ (plasmonic mode part), resulting in a maximum $Q$ factor under a certain ring radius $R_r$. Considering almost linear relationship between mode volume and ring radius $R_r$, i.e. increased mode volume with the increase in ring radius $R_r$, there exists an optimized ring radius $R_r$ to achieve the highest Purcell factor and the lowest threshold gain.

Furthermore, the proposed structure can be further engineered to be applicable for lasing applications at different wavelength bands. Either the high-index nanowire or the low-index gap layer can be considered as the gain medium region, offering more flexibility to facilitate desired lasing wavelength bands. As shown in Fig. 3(b), the available resonance wavelength can be extended in the near-infrared band regardless of lasing wavelength range of gain material. That is, one may choose other appropriate gain materials with specific lasing wavelength range to enable a flexible ring resonator laser operating at desired wavelength band. From Fig. 3(b), it is found that the upper limit of resonance wavelength behaves in a linear relationship with respect to the cross section radius $R_c$. The upper limit of resonance wavelength under a given cross section radius $R_c$ is corresponding to the lower limit of azimuthal mode number of HP and PH modes, which is a result of the minimum effective refractive index that can be achieved, as shown in Fig. 3(a). The general approach getting results in Fig. 3(a) and (b) indicates helpful design rules to choose proper gain materials and cross section radius $R_c$ according to the desired lasing applications.

Benefiting from the round-trip whispering-gallery-like mode properties, the designed active hybrid plasmonic ring resonator structure can avoid the undesired loss due to imperfect reflection at end-facets of previously reported straight plasmon laser structure with Fabry-Pérot-like cavity. Hence, active hybrid plasmonic ring resonator is expected to greatly improve the $Q$ factor. However, how to efficiently collect and output light from the ring resonator appears to be a challenge. Spiral structure could be a possible solution with detailed performance evaluation on the way to be carried out[15]. Moreover, the whole footprint of the proposed active hybrid plasmonic ring resonator is pretty small (sub-micron size), showing a potential ultra-compact lasing solution.

## Method

In cylindrical coordinates, the $m^{th}$-order whispering-gallery-like mode in the proposed ring resonator structure takes the form

$$\mathbf{\Psi}_m(\mathbf{r},\phi,\mathbf{z}) = \mathbf{C}_m\mathbf{\Phi}_m(\mathbf{r},\mathbf{z})e^{im\phi - i\omega t} \tag{1}$$

In this expression, the azimuthal mode number $m$ denotes the number of field maxima along the circumference of the ring resonator, $r$ is the radial distance from the center of ring resonator, $\Phi$ is the azimuthal angle, $\omega$ is the angular frequency, $\mathbf{C}_m$ is a coefficient, and $\mathbf{\Phi}_m(\mathbf{r},\mathbf{z})$ is the field profile at the cross section which satisfies the following equation

$$\nabla^2_{r,z}\mathbf{\Phi}_m(r,z) - m^2\mathbf{\Phi}_m(r,z) + \varepsilon\left(\frac{\omega}{c}\right)^2\mathbf{\Phi}_m(r,z) = 0 \tag{2}$$

where $\boldsymbol{\varepsilon}$ is the relative permittivity[16] and $c$ is the light velocity in vacuum. Using finite-element method and applying partial differential equation in a commercially available software COMSOL MULTIPHYSICS, the eigenfrequency $\omega_{eig}$ can be calculated, and then the wavelength resonance of the resonator is achieved by $\boldsymbol{\lambda} = 2\pi\mathbf{c}/\omega_{eig}$.

The $Q$ factor is obtained by

$$\mathbf{Q} = |\omega_{re}/2\omega_{im}| \tag{3}$$

where $\omega_{re}$ and $\omega_{im}$ are the real part and the imaginary part of the eigenfrequency $(\omega_{eig} = \omega_{re} + i * \omega_{im})$ of the ring resonator, respectively. The details of the whole calculation process can be found as an full-vector finite-element eigenfrequency solver for axis-symmetric structures[17].

Mode volume ($V$) is calculated by

$$\mathrm{V} = \left[\iiint W(\vec{r})d^3(\vec{r})\right] / W(\vec{r})_{max} \tag{4}$$

$$W(\vec{r}) = \frac{1}{2}\left[Re\left[\frac{d\{\varepsilon(\vec{r})\omega\}}{d\omega}\right]|\vec{E}(\vec{r})|^2 + \mu|\vec{H}(\vec{r})|^2\right] \tag{5}$$

where $W(\vec{r})$ is the energy density.

Purcell factor ($F_p$) is a figure of merit to represent the ability of a cavity for spontaneous emission enhancement. It is calculated by

$$F_p = \frac{3}{4\pi^2}\left(\frac{\lambda}{n_{eff}}\right)^3\left(\frac{Q}{V}\right) \quad (6)$$

where λ is the resonance wavelength, Q is the $Q$ factor, $V$ is the mode volume, and $n_{eff}$ is the effective refractive index of the ring resonator given by $n_{eff} = \frac{m\lambda}{2\pi R_r}$, where $m$ is the azimuthal mode order of the whispering-gallery-like mode, and $R_r$ is the ring radius of the resonator[18,19].

Considering the absorption loss by the metal substrate and the complicated hybrid mode properties of the designed hybrid plasmonic ring resonator, the estimation of the threshold gain from an effective optical length is not applicable. Instead, the proper way to assess the threshold gain ($G_{th}$) for a possible whispering-gallery-like mode is to use the following formula[13,20]

$$G_{th} = \frac{2\pi n_{eff}}{\Gamma_{gain}\lambda Q} \quad (7)$$

where $Q$ factor indicates the loss properties of a certain lasing mode and $\Gamma_{gain}$ is the energy confinement factor of the gain medium (the gain medium is CdS nanowire in the proposed ring resonator structure).


1. Rong, H., Liu, A., Jones, R., Cohen, O. & Hak, D. An all-silicon Raman laser. *Nature* **433**, 292–294 (2005).
2. Oulton, R. F. *et al.* Plasmon lasers at deep subwavelength scale. *Nature* **461**, 629–32 (2009).
3. Kogelnik, H. & Li, T. Laser beams and resonators. *Proceedings of the IEEE* **54**, 1312–1329 (1966).
4. Vahala, K. Optical microcavities. *Nature* **424**, 839–846 (2003).
5. Gramotnev, D. K. & Bozhevolnyi, S. I. Plasmonics beyond the diffraction limit. *Nature Photonics* **4**, 83–91 (2010).
6. Hill, M. T. *et al.* Lasing in metallic-coated nanocavities. *Nature Photonics* **1**, 589–594 (2007).
7. Noginov, M. a. *et al.* Demonstration of a spaser-based nanolaser. *Nature* **460**, 1110–2 (2009).
8. Oulton, R. F., Sorger, V. J., Genov, D. a., Pile, D. F. P. & Zhang, X. A hybrid plasmonic waveguide for subwavelength confinement and long-range propagation. *Nature Photonics* **2**, 496–500 (2008).
9. Xiao, Y.-F. *et al.* High quality factor, small mode volume, ring-type plasmonic microresonator on a silver chip. *Journal of Physics B: Atomic, Molecular and Optical Physics* **43**, 035402 (2010).
10. Johnson, P. & Christy, R. Optical constants of the noble metals. *Physical Review B* **1318** (1972).
11. Zhu, L. Modal Properties of Hybrid Plasmonic Waveguides for Nanolaser Applications. *IEEE Photonics Technology Letters* **22**, 535–537 (2010).
12. Agarwal, R., Barrelet, C. J. & Lieber, C. M. Lasing in single cadmium sulfide nanowire optical cavities. *Nano letters* **5**, 917–20 (2005).
13. Gargas, D. J. *et al.* Whispering gallery mode lasing from zinc oxide hexagonal nanodisks. *ACS nano* **4**, 3270–6 (2010).
14. Cheng, P., Weng, C. & Chang, S. Plasmonic gap-mode nanocavities with metallic mirrors in high-index cladding. *Optics Express* **21**, 629–632 (2013).
15. Poon, A., Luo, X. & Chen, H. Microspiral resonators for integrated photonics. *Optics and Photonics News* **19**, 48–53 (2008).
16. Chen, Y., Zou, C., Hu, Y. & Gong, Q. High- Q plasmonic and dielectric modes in a metal-coated whispering-gallery microcavity. **023824**, 1–9 (2013).
17. Oxborrow, M. Traceable 2D finite-element simulation of the whispering-gallery modes of axisymmetric electromagnetic resonators. *IEEE Trans. Microw. Theory and Tech.* **55**, 1209–1218 (2007).
18. Ellis, D. J. P. *et al.* Cavity-enhanced radiative emission rate in a single-photon-emitting diode operating at 0.5 GHz. *New Journal of Physics* **10**, 043035 (2008).
19. Min, B. *et al.* High-Q surface-plasmon-polariton whispering-gallery microcavity. *Nature* **457**, 455–8 (2009).
20. Chang, S.-W. & Chuang, S. L. Fundamental Formulation for Plasmonic Nanolasers. *IEEE Journal of Quantum Electronics* **45**, 1014–1023 (2009).


## Acknowledgments

This work was supported by the National Natural Science Foundation of China (NSFC) under grants 61222502 and 61077051, and the Program for New Century Excellent Talents in University (NCET-11-0182).

## Author contributions

C.X. and J.W. developed the concept and conceived the design. C.X. performed the numerical simulations. J.W. analyzed the data. C.X., J.W. and C.C. contributed to writing and finalizing the paper.

## Additional information

**Competing financial interests:** The authors declare no competing financial interests.

**How to cite this article:** Xiang, C., Chan, C.-K. & Wang, J. Proposal and numerical study of ultra-compact active hybrid plasmonic resonator for sub-wavelength lasing applications. *Sci. Rep.* **4**, 3720; DOI:10.1038/srep03720 (2014).